

Thermal and Thermomechanical Properties of Poly(ethylene oxide) Networks Produced with Silica and Organic Crosslinking Agents

Jung-Ohk Kweon, Si-Tae Noh

Department of Chemical Engineering, Hanyang University, 1271, Sa Dong, Ansan City, Kyunggi-do, 425-791, Korea

Received 15 September 2001; accepted 17 January 2003

ABSTRACT: The thermal and thermomechanical properties of two series of poly(ethylene oxide) networks (NPEOs) were investigated as a function of the chain length between crosslink sites (M_c) and the concentration of LiClO_4 (C_L) in the NPEOs. The two series of networks were produced with silica and organic crosslinking agents and, therefore, had crosslink sites of different natures: one was an inorganic silicate network (silica NPEO), and the other was an organic polar group (organic NPEO). The crosslink sites in both series of networks were commonly covalently bonded to the poly(ethylene oxide) (PEO) phase through a urethane group in the NPEOs. The glass-transition temperatures (T_g 's) of the PEO phases in the NPEOs, according to differential scanning calorimetry, increased with a decrease in M_c and were higher in the silica NPEOs than in the organic NPEOs under the same M_c conditions. The difference in T_g between the two series of networks with the same M_c values increased with decreasing M_c . These results suggested that the interaction of crosslink sites with the PEO phase was stronger in the silica NPEOs than in the organic NPEOs. The addition of LiClO_4 to the NPEOs resulted in T_g of the PEO phase in the

NPEOs being elevated and increased according to the increase in C_L . The increase of T_g of the PEO phase according to the increase of C_L in the NPEOs was retarded or saturated at high values of C_L , and this indicated that the limit of solubility of the salt in the polymer was attained. The retardation or saturation of the increase of T_g was also observed in dynamic mechanical analyses. The curves of the loss factor $\tan \delta$ and temperatures from the dynamic mechanical analyses for the NPEOs with high values of C_L showed shoulders or double peaks indicating the existence of the second phase in the polymer networks. In the curves of $\tan \delta$ for salt-complexed NPEOs with high values of C_L , silica NPEOs showed a shoulder of low intensity, but organic NPEOs showed a distinguished second peak becoming stronger with increasing C_L . The results of the T_g behavior and $\tan \delta$ curves suggested that the salt solubility in the NPEOs was limited and that the salt solubility of PEO in the silica NPEOs was higher than that in the organic NPEOs. © 2003 Wiley Periodicals, Inc. *J Appl Polym Sci* 90: 270–277, 2003

Key words: networks; silicas; thermal properties

INTRODUCTION

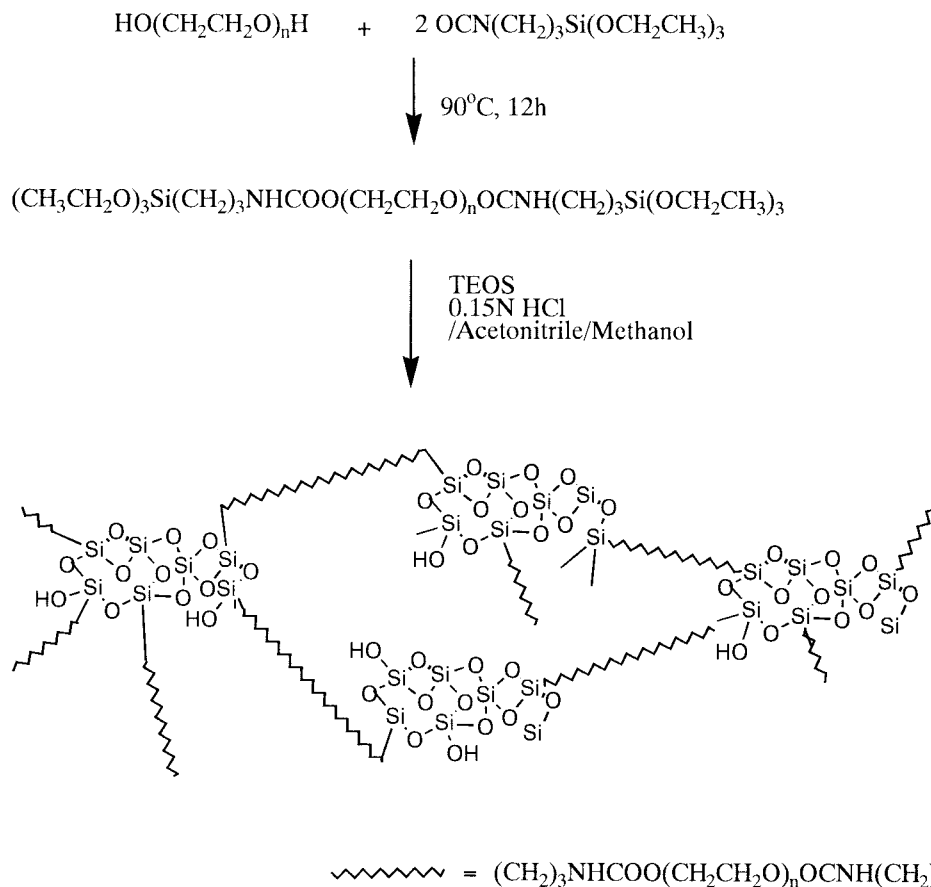
Lithium-ion-conducting solid polymer electrolytes have received considerable attention because of the desire for high-energy-density secondary batteries that can be used in a wide range of applications, from consumer electronics to electric vehicles. Poly(ethylene oxide) (PEO) is the most interesting base material for hosting lithium salts because PEO contains ether coordination sites, which assist with the dissociation of salts incorporated into the polymer, and a flexible macromolecular structure, which promotes facile ionic transport.^{1,2} Ionically conducting polyether-based networks containing alkali-metal salts were researched during the past decade because improved mechanical properties and ion-conducting properties due to the lower crystallinity of the materials were expected, in comparison with the behavior of linear polyethers.² It

is generally known that the nature of the crosslinks influences the properties of the networks.^{3–5}

Inorganic salts can be dissolved in hybrid networks of silica PEO, and this results in good ionic conductors.^{6–8} Hybrid networks of PEO derived from the *in situ* sol–gel reaction of PEO functionalized with trialkoxy silane consist of organic (polymer) and inorganic (silica) phases linked together through covalent bonds. In the hybrid materials, the two phases are mixed on a nanometric scale and have a very high surface-to-volume ratio, leading to materials with new properties such as transparency and high mechanical strength.^{6,9–13} Fujita and Honda⁷ reported hybrid polymer electrolytes based on silica PEO consisting of inorganic oxide and organic components interconnected through covalent bonds. Bonagamba et al.⁸ reported an NMR study of an ion-conducting organic–inorganic nanocomposite, PEO–silica– LiClO_4 .

Such hybrid networks with inorganic hard clusters differ from networks derived from the other organic reaction in several ways: (1) the inorganic clusters are harder and do not soften in the normal temperature range; (2) the inorganic clusters are usually less mis-

Correspondence to: S.-T. Noh (stnoh@ihanyang.ac.kr).
Contract grant sponsor: Korea Research Foundation.



Scheme 1 Preparation of silica NPEOs.

cible with the organic continuous phase; and (3) the inorganic (silica) clusters contain some silanol groups strongly interacting with polar groups of the organic components, even if in polyurethanes the urethane groups are also active in hydrogen bonding.³ These special features of the inorganic phase at a junction point of networks can lead to properties distinguishable from those of the networks prepared from the other organic reaction. Several studies on the influence of the nature of the crosslinking points on the properties of network polymers have been reported.³⁻⁵ However, the effect of inorganic hard clusters, distinguished from that of organic clusters, on the properties of network polymer electrolytes has rarely been researched.

In this study, we investigated the effect of inorganic hard clusters on the thermal and thermomechanical properties of poly(ethylene oxide) networks (NPEOs) and their lithium salt complexes. The thermal and thermomechanical properties affect the chain mobility and phase behaviors of polymeric materials; these are important properties related to the ion-conducting properties of polymer electrolytes. For this reason, we investigated the properties of two series of NPEOs that were similar to each other, except that they had different internal structures of the crosslink sites

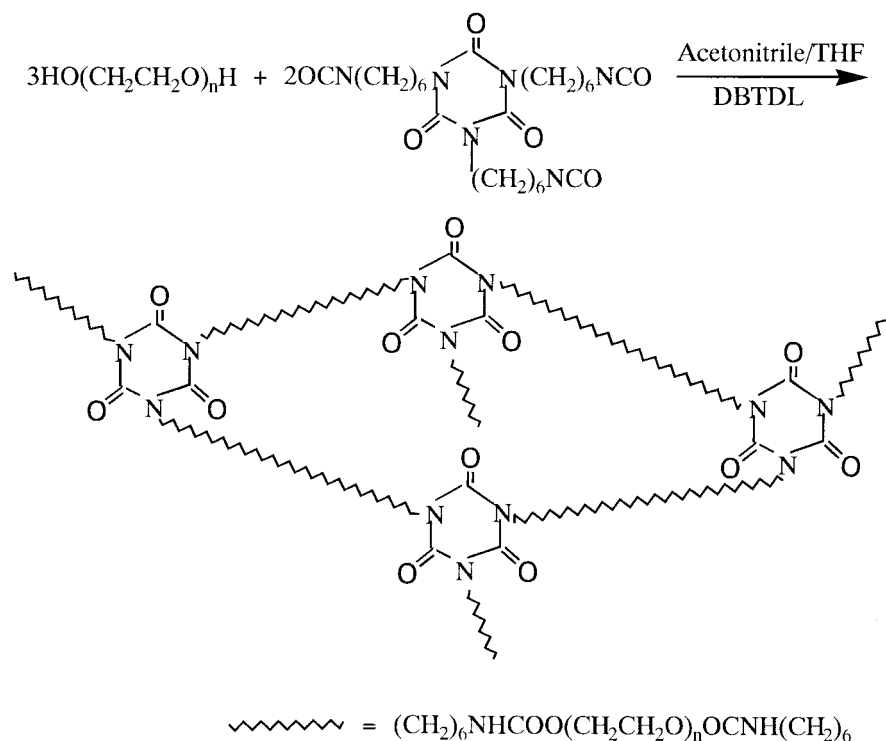
bonded to the PEO phase through urethane groups. In the internal structures of the crosslinks, one series of networks had an inorganic phase of a silicate network (silica NPEO), and the other had an organic polar group (organic NPEO). Two types of networks with the same chain length between crosslinking points (M_c) were designed to have similar weight fractions of the crosslink parts. The thermal and thermomechanical properties of the two types of NPEOs were investigated as a function of M_c and the concentration of LiClO_4 (C_L) in NPEO/ LiClO_4 complexes with differential scanning calorimetry (DSC) and dynamic mechanical analysis (DMA).

EXPERIMENTAL

Materials

PEO diols (Shinyo Pure Chemicals Co., Ltd., Osaka, Japan) with number-average molecular weights (M_n 's) of 600, 1000, and 2000 (determined by OH titration) were used. The PEO diols were dried under reduced pressure at 80°C for 8 h just before use.

A series of salt-free or salt-complexed silica NPEOs were prepared by the sol-gel processes described else-



Scheme 2 Preparation of organic NPEOs.

where¹⁴ (Scheme 1). The existence of covalent chemical bonds between the silica network and the polymer chains has been reported for similar materials.^{6,12,15} The weight fractions of the crosslink parts of the silica NPEOs were adjusted to those of the organic NPEOs through the amount of added tetraethoxysilane (TEOS), which was used as a coprecursor for the sol-gel reaction. These networks were designated SM_Li(X), where *M* represents the number-average molecular weight of the PEO diol and *X* represents the [EO]/[Li⁺] molar ratios (0, 4, 8, 12, 16, or 24).

The organic NPEOs were prepared from the dibutyl tin dilaurate (DBTDL)-catalyzed urethane reaction of ½ mol of PEO diol and ⅓ mol of tris(6-isocyanatohexyl)isocyanurate in an acetonitrile/tetrahydrofuran (THF) solution, as shown in Scheme 2. The transparent acetonitrile/THF solution of the PEO diol and tris(6-isocyanatohexyl)isocyanurate was well mixed for 5 h at room temperature, poured onto a Teflon plate, and cured for 12 h at 70°C. The salt-complexed organic NPEOs were prepared by the same process used for the salt-free organic NPEOs, except for the addition of an acetonitrile solution of lithium perchlorate (LiClO₄; 95%; Aldrich, USA) to the reaction solution. These products were dried under reduced pressure at 80°C for 24 h. These were designated OM_Li(X), where *M* represents the number-average molecular weight of the used diol and *X* represents the [EO]/[Li⁺] molar ratio (0, 4, 8, 12, 16, or 24).

Measurements

The sol content in the salt-free PEO-based networks was determined by extraction at room temperature in THF. After 1 week, the extracted polymer was dried, and its mass was determined. The sol fraction (*w_s*) was calculated with the following relation:

$$w_s = 100(1 - w_d/w_0) \quad (1)$$

where *w_d* is the mass of the dry residue and *w₀* is the initial mass of the polymer.

Absorbance spectra were obtained with a Golden Gate Diamond attenuated-total-reflection Fourier transform infrared (ATR-FTIR) immersion probe attached to a Nicolet Protege 460 FTIR spectrophotometer connected to a 333-MHz Pentium II running Omnic 4.1a software from Nicolet Instrument Corp. The spectrometer was purged with N₂ gas 1 h before, while measurements were being taken, to reduce the effects of CO₂ absorption in its optical path. A spectral resolution of 4 cm⁻¹ was used as a compromise between scan speed and resolution. Thermogravimetric analysis (TGA; Shimadzu TGA-50) was carried out from room temperature to 900°C at a heating rate of 10°C/min under a nitrogen atmosphere. DSC (DSC2010, TA Instrument) was carried out with annealing at 65°C for 15 min, slow cooling to -100°C, and scanning to 200°C at a heating rate 10°C/min

under nitrogen. The glass-transition temperatures (T_g 's) were determined as the midpoint of the phase-transition-temperature region in the DSC thermograms. Thermomechanical measurements were performed with a dynamic mechanical analyzer (DMA 2980, TA Instrument) operating in the film tension mode. The temperature dependence of the dynamic mechanical properties was measured in the range of -100 to 100°C at a heating rate of $2^\circ\text{C}/\text{min}$ and at a constant frequency of 5 Hz .

RESULTS AND DISCUSSION

The preparation conditions, such as the reaction media and curing times and temperatures, for the salt-free NPEOs were fixed, and this resulted in networks with sol fractions below approximately 1%. The salt-complexed NPEOs were prepared under the same conditions as the salt-free NPEOs. The network formation of salt-complexed networks was confirmed with ATR-FTIR, TGA, and DSC. The TGA results for the prepared networks showed that the weight loss of the networks by heating did not appreciably start until 110°C , indicating that the residual solvent in the networks was negligible. Figure 1 shows the absorption band spectra obtained by ATR-FTIR for some of the networks studied. The absorption band at 2270 cm^{-1} ,

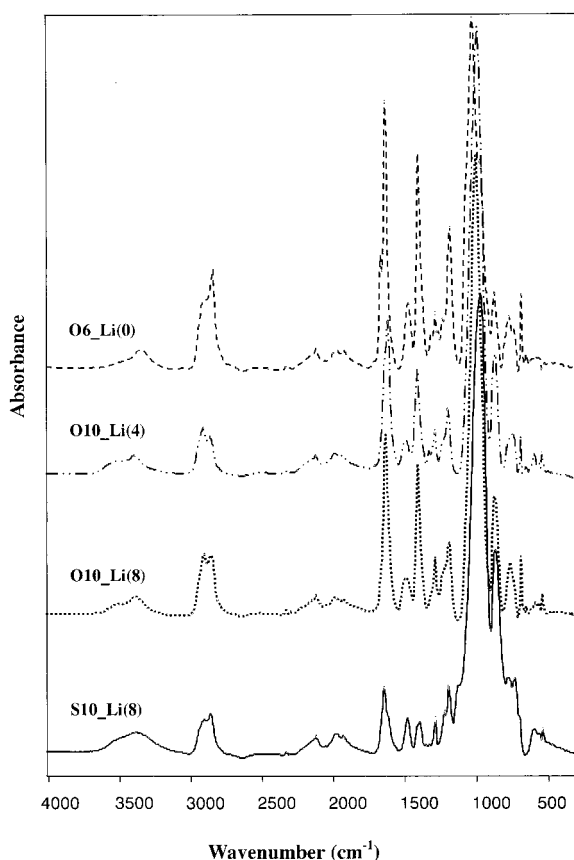


Figure 1 ATR spectra of the studied networks.

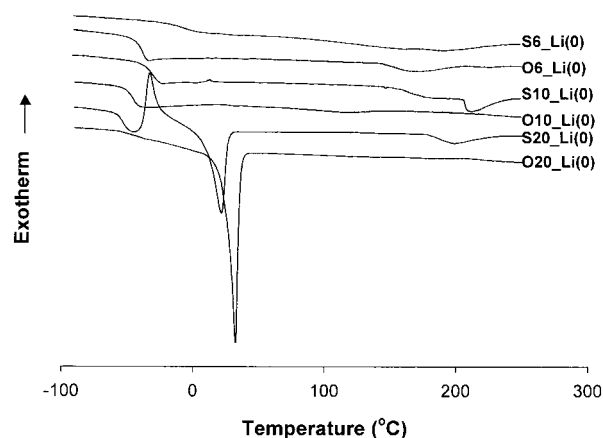


Figure 2 DSC thermograms of the salt-free networks.

corresponding to unreacted isocyanate, was not observed in salt-free organic NPEOs [O6_Li(0)] or salt-complexed organic NPEOs with high salt contents [O10_Li(4) and O10_Li(8)]. Low sol fractions and the results of ATR-FTIR analyses indicated that, in both salt-free and salt-complexed organic NPEOs, the amount of the residue of the unreacted hydroxyl and isocyanates group was negligible. In the ATR-FTIR spectra of the silica NPEO S10-Li(8), the characteristic absorption band for the silicate network of Si—O stretching) was not distinguished because of overlap with the others. A broad endotherm starting at 50 – 100°C in the DSC thermograms of silicate networks prepared by the sol–gel process could be observed, and it was attributed to the evolution of the solvents, reactant, adsorbed water, and products arising from the further condensation of incompletely condensed inorganic species.¹⁶ However, the broad endotherm at 50 – 100°C in the DSC thermograms of the silica NPEOs was hardly observed, as shown in Figure 2. The results suggested that the existence of the residual solvents, reactant, absorbed water, and incompletely condensed inorganic species in the prepared silica NPEOs was negligible. The endotherm was also not observed in the salt-complexed silica NPEOs.

Thermal properties

DSC measurements allowed us to characterize the thermal properties, such as the melting temperature (T_m), corresponding to the melt of the crystalline phase (ΔH), and T_g , which strongly influenced the ion-conducting properties of the solid polymer electrolytes. PEO is a highly crystalline polymer because of its highly stereoregular structure, having no chain branching and containing highly polar ether groups that give rise to very strong dipole–dipole interactions. The thermal parameters from DSC studies of PEO diols with $M_n = 2000$ were as follows: $T_m = 54^\circ\text{C}$,

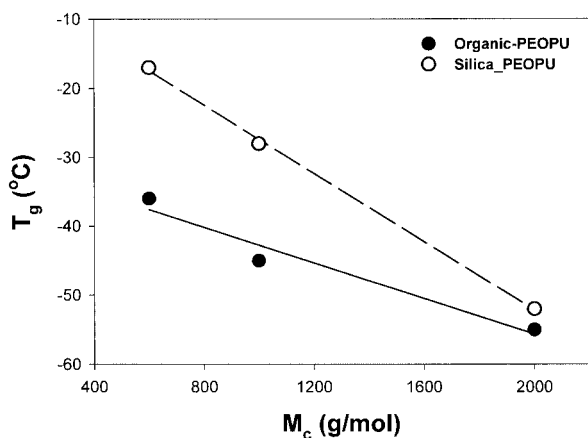


Figure 3 Variations of T_g as a function of M_c for the salt-free networks.

degree of crystallinity [i.e., the crystalline weight fraction (w_c), as judged by the specific volume] = 0.89, and $\Delta H = 181$ J/g. These results are agree well with those of a previous report.¹⁷

Figure 2 shows the DSC curves for the salt-free NPEOs. The results of Figure 2 indicate that the thermal behaviors of the PEO phase in the NPEOs were strongly influenced by the properties of the internal structures of the crosslink sites and M_c . The DSC curves for both types of salt-free NPEOs with $M_c = 2000$ showed endothermic peaks corresponding to the melting of the PEO phase. The parameters corresponding to the crystalline behavior of PEO in the NPEOs with $M_c = 2000$ were lowered as follows: for silica NPEO, T_m was 22°C, ΔH was reduced to 36 J/g, and w_c was reduced to 0.19, and, for organic NPEO, T_m was 35°C, ΔH was reduced to 61 J/g, and w_c was reduced to 0.31. These changes in the crystalline properties of PEO in NPEOs were due to the existence of a junction point disturbing the crystalline formation and acting as a crystalline defect and due to the interaction between the PEO chain and junction part disturbing the crystalline formation. Lower thermal parameters of PEO in silica NPEOs than in organic NPEOs were observed, indicating that the crystalline formation of PEO chains was more strongly suppressed in silica NPEOs than in organic NPEOs. This result suggests that the internal structure of silica NPEOs was more effective in the suppression of the crystalline formation of PEO chains than that of organic NPEOs. An endotherm due to the crystalline phase of PEO was not observed in DSC curves of silica NPEOs and organic NPEOs with $M_c = 1000$ or 600. This can be explained by the suppression of crystallinity, which was brought about by an increase in the concentration of crosslinks, resulting in lower M_c values.

T_g of the PEO phase in the NPEOs was shifted to higher temperatures according to the decrease of M_c , and this resulted in an increase in the crosslinking

density, as shown in Figure 2. This could be explained by the fact that the most severe mechanism for decreasing molecular freedom was chemical crosslinking: linking the polymer chains together through covalent or ionic bonds to form a network.¹⁸ The effect of M_c and the internal structures of the crosslink sites on T_g of the PEO phase in the NPEOs can be seen in Figure 3, which presents plots of M_c and T_g of the PEO phase in salt-free NPEOs. Figure 3 shows that the NPEO with the lower M_c and the higher crosslink density had the higher T_g and that the T_g 's of the PEO phases in the silica NPEOs were higher than those in the organic NPEOs. The difference in T_g between the two types of NPEOs with the same M_c increased with decreasing M_c and an increasing weight fraction of the crosslink part. This indicated that T_g of the PEO phase in the NPEOs depended on not only the crosslink density but also the internal structure of the crosslink parts and that the mobility of PEO chains in NPEOs with silica nodes in the crosslinks was more restricted than in the network with polar organic nodes. It was previously known from the study of NPEOs with urethane or cyclosiloxane crosslinks⁴ that the nature of the internal structure of the crosslinks of the networks influenced the local dynamics of NPEOs. The higher T_g and lower crystallinity of the PEO phase in silica NPEOs could be explained by the harder properties of silica and the existence of silanol ($-\text{SiOH}$), which interacted with the ether part of PEO through the hydrogen bonding. Similar effects were also observed for a nonbonded silica-PEO hybrid and PEO intercalated in clays.^{8,19}

The effect of added salt on T_g of the PEO phase in NPEOs can be seen in Figure 4, which shows T_g 's obtained from DSC as a function of the $[\text{Li}^+]/[\text{EO}]$ molar ratios for the two systems with $M_c = 1000$. Figure 4 indicates that the higher mobility of the PEO phase in silica NPEOs with respect to organic NPEOs

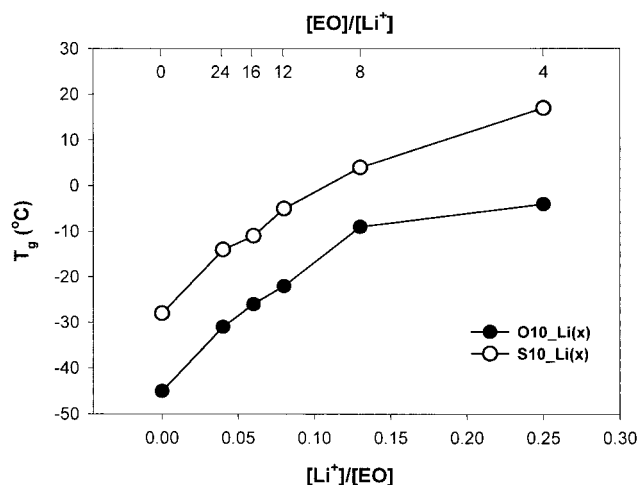


Figure 4 Variations of T_g as a function of the added salt content for the salt-complexed networks with $M_c = 1000$.

was also observed under the salt-complexed state. T_g of the PEO phase in the salt-complexed NPEOs was higher than that of the salt-free polymers. An increase in T_g of the salt-complexed polyether system was generally observed and was due to the dipole-cation interactions between polyether segments and dissociated ions, that is, lithium ions.²⁰ The cation-dipole interactions were due to ionic bonding and might have acted as transient crosslink points in the polymer electrolytes. This largely reduced the segmental mobility of polyether and occurred with an increase in T_g . The increase of T_g became slightly retarded above C_L ($[\text{Li}^+]/[\text{EO}] = 0.13$ ($[\text{EO}]/[\text{Li}^+] = 8$). T_g 's of most of the polyether-salt complexes reached limiting values at high salt concentrations. It is apparent that these values were achieved when the limit of solubility limited the existence of more salt as a second phase and produced no further elevation of T_g . Below this limit, the salt was believed to be molecularly dispersed in the polymer.¹⁹

Thermomechanical properties

Figure 5 shows storage modulus (E') and temperature curves at 1 Hz for the salt-free NPEOs. For all networks, a rubberlike plateau in E' above T_g was observed. The width of the glass transition was related to the distribution of relaxation times and, therefore, to the degree of homogeneity in the samples.²¹ Measurements of the transition width were made by the observations of changes in the full width at half-maximum of the $\tan \delta$ peak shown in Figure 5. The half-width at full maximum for silica NPEO with $M_c = 1000$ was 8, and for the one with $M_c = 600$, it was 13. The half-width at full maximum for organic NPEO with $M_c = 1000$ was 11, and for the one with $M_c = 600$, it was 26. The width of the $\tan \delta$ peak of NPEO with a low value of M_c became broader than that with a high value of M_c . Under the same M_c state, silica NPEOs had broader $\tan \delta$ peaks than organic NPEOs. It is suggested that the properties and amount of the junction point influenced the distribution of relaxation times in the polymer and that the silicate node was more interactive with PEO chains than the organic polar groups. These DMA results agreed well with the aforementioned DSC results.

The plots in Figures 6 and 7 show the dynamic mechanical spectra at various salt concentrations for silica NPEOs and organic NPEOs, respectively. For all samples, a rubberlike plateau in E' above T_g was also observed, indicating the network structures. In the DMA curves, the salt-free samples with $M_c = 1000$ displayed a single T_g , and this suggested that, on the length scale probed by DMA (100 Å), the samples consisted of a single phase.²² In both types of NPEOs, the $\tan \delta$ peaks for the NPEOs with C_L greater than $[\text{Li}^+]/[\text{EO}] = 0.13$ ($[\text{EO}]/[\text{Li}^+] = 8$) exhibited two

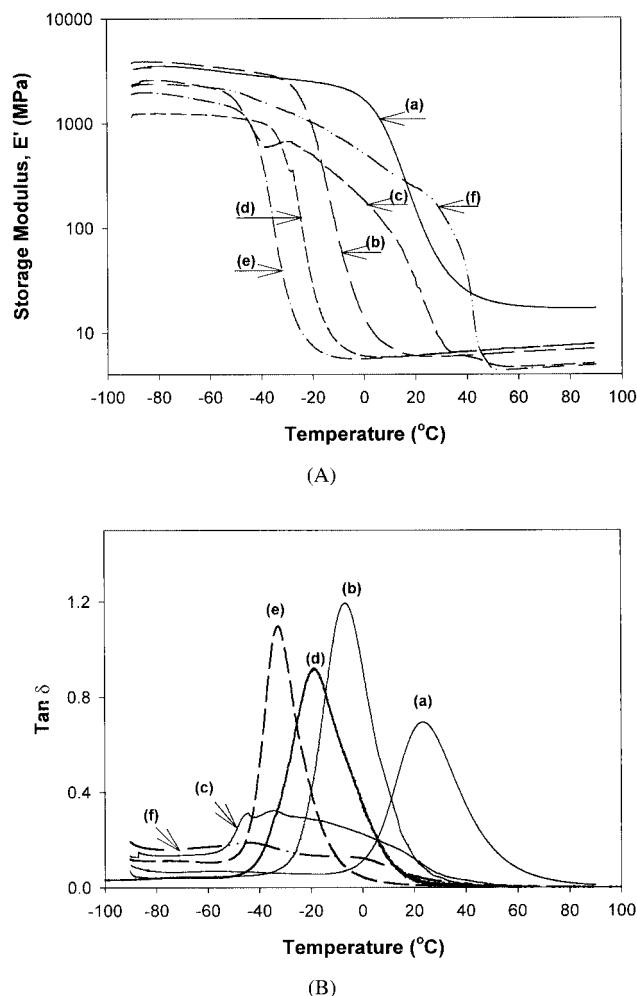


Figure 5 DMA curves of the salt-free networks: (A) E' versus temperature and (B) $\tan \delta$ versus temperature: (a) S(6)_Li(0), (b) S10_Li(0), (c) S20_Li(0), (d) O(6)_Li(0), (e) O10_Li(0), and (f) O20_Li(0).

peaks or a shoulder toward the low temperature. This suggested that both types of NPEOs with high values of C_L had two heterogeneous phases. In the salt-complexed NPEOs with high values of C_L producing no further elevation of T_g , above the limit of solubility, more salt existed as a second phase, as suggested by the DSC results. The two peaks could be associated with a salt-aggregated phase and a salt-dissolved phase. Observations consistent with the formation of salt-rich phases as the salt concentration was increased were also made for poly(propylene oxide) (PPO)/ LiClO_4 and amorphous PEO1000/ LiClO_4 complexes.²³⁻²⁵ For the organic NPEOs, the intensity of the $\tan \delta$ peak at lower temperatures increased with a rising salt concentration. For the silica NPEOs, the $\tan \delta$ peak with a shoulder of the networks with $[\text{Li}^+]/[\text{EO}] = 0.13$ ($[\text{EO}]/[\text{Li}^+] = 8$) became split into two peaks for the sample with $[\text{Li}^+]/[\text{EO}] = 0.25$ ($[\text{EO}]/[\text{Li}^+] = 4$). These results indicated that the peak at the lower temperature corresponded to the second phase, a salt-

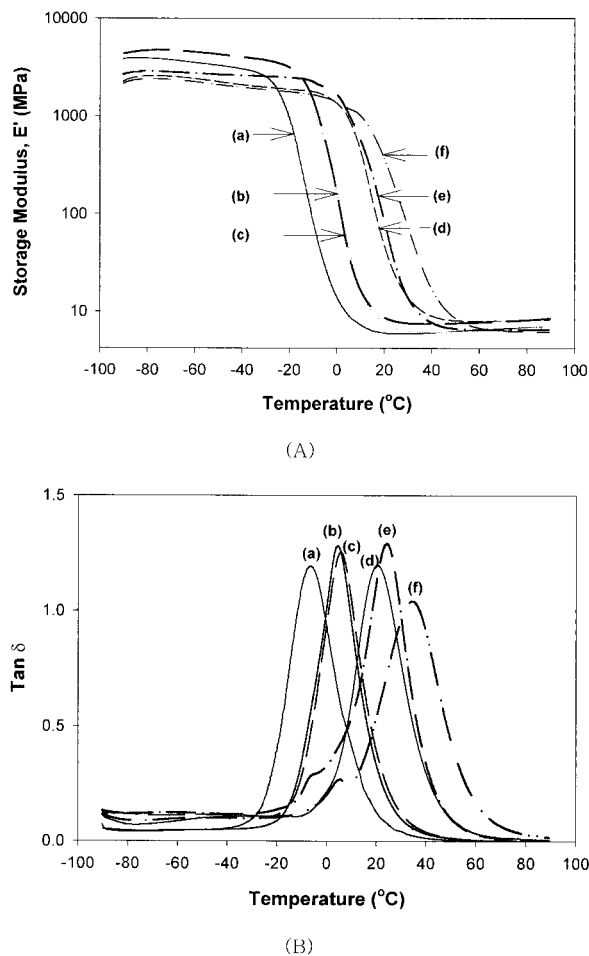


Figure 6 DMA curves of the salt-complexed S10_Li(X) networks: (A) E' versus temperature and (B) $\tan \delta$ versus temperature: (a) S10_Li(0), (b) S10_Li(24), (c) S10_Li(16), (d) S10_Li(12), (e) S10_Li(8), and (f) S10_Li(4).

aggregated phase. The intensity of the second peak of the organic NPEOs was higher than that of the silica NPEOs. This means that more of the second phase was formed in the organic NPEOs than in the silica NPEOs, and it reinforces the preceding conclusions from DSC analysis: the salt solubility of the silica NPEOs was higher than that of the organic NPEOs.

It has been reported that polar and hydrogen-bond groups such as urethane contribute to increasing the dielectric constant of a system²⁶ and to generating more dissociated ions.⁵ In water or hydrogen-bonded solvents such as alcohols, the anions are solvated and thereby stabilized by the hydrogen bonds.²⁷ Both the silica NPEOs and organic NPEOs had urethane groups that could form hydrogen bonds with oxygen in salt anions (ClO_4^-). However, the silica NPEOs could form additional hydrogen bonds via silanol groups ($-\text{SiOH}$), and so the stabilization effect of the anion in these networks was larger than in the organic networks (organic NPEOs). This could explain the higher solubility of salts in the silica NPEOs than in PEO or others.

CONCLUSIONS

NPEOs with silica in the crosslink sites had thermal and thermomechanical properties distinguishable from those of networks with organic polar groups in the crosslink sites. The PEO phase in the silica NPEOs had lower crystalline properties and chain mobility than that in the organic NPEOs. This tendency was kept in the salt-complexed networks. Both salt-complexed NPEOs showed a limit of solubility, as suggested by DSC results, and exhibited a second phase associated with a salt-aggregated phase at lower temperature, as suggested by $\tan \delta$ and temperature curves exhibiting two peaks. The salt solubility of the silica NPEOs was higher than that of the organic NPEOs, as suggested by $\tan \delta$ and temperature curves and T_g and salt-content curves. The higher stabilization properties of salt anions and the more polar properties of the silica node, with respect to the organic node, could be explained by the greater solubility of the salt in the silica NPEOs than in PEO or others.

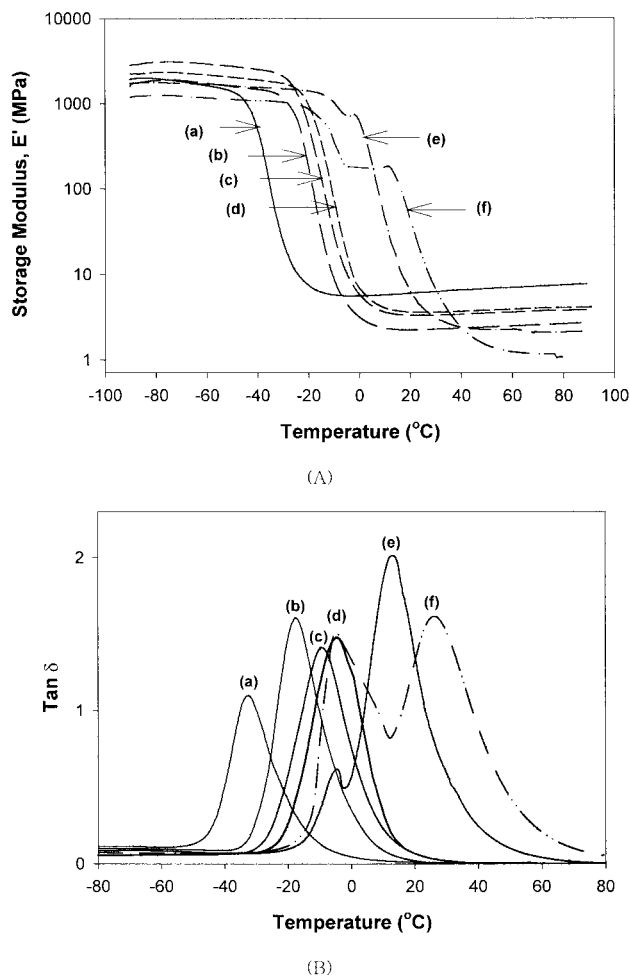


Figure 7 Dynamic mechanical spectra of the salt-complexed O10_Li(X) networks: (A) E' versus temperature and (B) $\tan \delta$ versus temperature: (a) O10_Li(0), (b) O10_Li(24), (c) O10_Li(16), (d) O10_Li(12), (e) O10_Li(8), and (f) O10_Li(4).

References

1. MacCallum, J. R.; Vincent, C. A. *Polymer Electrolyte Review*; Elsevier: London, 1987 and 1989; Vols. 1 and 2.
2. Tonge, J. S.; Shriver, D. F. In *Polymers for Electronic Applications*; Lai, J. H., Ed.; CRC: Boca Raton, FL, 1989; p 194.
3. Cuney, S.; Gérard, J. F.; Dumon, M.; Pascault, J. P.; Vigier, G.; Dušek, K. *J Appl Polym Sci* 1997, 65, 2373.
4. Lestel, L.; Guégan, P.; Boileau, S.; Cheradame, H.; Lauprêtre, F. *Macromolecules* 1992, 25, 6024.
5. Yoon, S.; Ichikawa, K.; MacKnight, W. J.; Hsu, S. L. *Macromolecules* 1995, 28, 5063.
6. Ravaine, D.; Seminel, A.; Charbouillot, Y.; Vincens, M. *J Non-Cryst Solids* 1986, 82, 210.
7. Fujita, M.; Honda, K. *Polym Commun* 1989, 30, 200.
8. Mello, N. C.; Bonagamba, T. J.; Panepucci, P.; Dahmouche, K.; Judeinstein, P.; Aegerter, M. A. *Macromolecules* 2000, 33, 1280.
9. Judeinstein, P.; Sanchez, C. *J Mater Chem* 1996, 6, 511.
10. Novac, B. M. *Adv Mater* 1993, 5, 422.
11. Judeinstein, P.; Titman, J.; Stamm, M.; Schmidt, H. *Chem Mater* 1994, 6, 127.
12. Brik, M. E.; Titman, J. J.; Bayle, J. P.; Judeinstein, P. *J Polym Sci Part B: Polym Phys* 1996, 34, 2533.
13. Schmidt, H.; Proppal, M.; Rousseau, F.; Poinsignon, C.; Armand, M.; Rousseau, J. Y. *Int Symp Polym Electrolytes* 1989, 2, 325.
14. Kweon, J. O.; Noh, S. T. *J Appl Polym Sci* 2001, 81, 2471.
15. Judeinstein, P.; Brik, M. E.; Bayle, J. P.; Courtieu, J.; Rault, J. *J Mater Res Soc Symp Proc* 1994, 346, 937.
16. David, I. A.; Scherer, G. W. *Chem Mater* 1995, 7, 1957.
17. Booth, C.; Nicholas, C. V.; Wilson, D. J. In *Polymer Electrolyte Review*; MacCallum, J. R.; Vincent, C. A., Eds., Elsevier: London, 1987; p 231.
18. Chompff, A. J.; Newman, S. *Polymer Networks: Structural and Mechanical Properties*; Plenum: New York, 1971.
19. Wong, S.; Vaia, R. A.; Gianellis, E. P.; Zax, D. B. *Solid State Ionics* 1996, 86, 547.
20. James, D. B.; Wetton, R. E.; Brown, D. S. *Polymer* 1979, 20, 187.
21. McCrum, N. G.; Buckley, C. P.; Bucknall, C. B. *Principles of Polymer Engineering*; Oxford Science: Oxford, 1991.
22. Utracki, L. A. *Polymer Alloys and Blends: Thermodynamics and Rheology*; Oxford Science: Oxford, 1988.
23. Watanabe, M.; Oohashi, S.; Sanui, K.; Ogata, N.; Kobayashi, T.; Ohtaki, Z. *Macromolecules* 1985, 18, 1945.
24. Killis, A.; Lenest, J. F.; Gandini, A.; Cheradame, H. *Macromolecules* 1984, 17, 63.
25. Ng Simon, T. C.; Forsyth, M.; MacFarlane, D. R.; Garcia, M.; Smith, M. E.; Strange, J. H. *Polymer* 1998, 39, 6261.
26. Ichikawa, K.; MacKnight, J. W. *Polymer* 1992, 33, 4693.
27. Gray, F. M. *Solid Polymer Electrolytes: Fundamentals and Technological Applications*; VCH: New York, 1991.